


Human Platelet Lysate Improves Bone Forming Potential of Human Progenitor Cells Expanded in Microcarrier-Based Dynamic Culture

PRIYANKA GUPTA,^{a,b} GABRIELLA NILSSON HALL,^{a,b} LIESBET GERIS,^{a,c,d} FRANK P. LUYTEN,^{a,b,*} IOANNIS PAPANTONIOU ^{a,b,*}

^aPrometheus, Division of Skeletal Tissue Engineering, KU Leuven, Leuven, Belgium; ^bSkeletal Biology and Engineering Research Center, KU Leuven, Leuven, Belgium; ^cBiomechanics Research Unit, GIGA-R In Silico Medicine, Université de Liège, Liège, Belgium; ^dBiomechanics Section, KU Leuven, Leuven, Belgium

*Co-senior authors.

Correspondence: Dr. Ioannis Papantoniou, Ph.D., Prometheus, Division of Skeletal Tissue Engineering, KU Leuven, O&N1 Herestraat 49, Leuven, Belgium. Telephone: +3216372743; e-mail: ioannis.papantoniou@med.kuleuven.be

Received October 4, 2018; accepted for publication March 19, 2019; first published April 30, 2019.

<http://dx.doi.org/10.1002/sctm.18-0216>

This is an open access article under the terms of the Creative Commons Attribution-NonCommercial-NoDerivs License, which permits use and distribution in any medium, provided the original work is properly cited, the use is non-commercial and no modifications or adaptations are made.

ABSTRACT

Xenogenic-free media are required for translating advanced therapeutic medicinal products to the clinics. In addition, process efficiency is crucial for ensuring cost efficiency, especially when considering large-scale production of mesenchymal stem cells (MSCs). Human platelet lysate (HPL) has been increasingly adopted as an alternative for fetal bovine serum (FBS) for MSCs. However, its therapeutic and regenerative potential in vivo is largely unexplored. Herein, we compare the effects of FBS and HPL supplementation for a scalable, microcarrier-based dynamic expansion of human periosteum-derived cells (hPDCs) while assessing their bone forming capacity by subcutaneous implantation in small animal model. We observed that HPL resulted in faster cell proliferation with a total fold increase of 5.2 ± 0.61 in comparison to 2.7 ± 0.22 -fold in FBS. Cell viability and trilineage differentiation capability were maintained by HPL, although a suppression of adipogenic differentiation potential was observed. Differences in mRNA expression profiles were also observed between the two on several markers. When implanted, we observed a significant difference between the bone forming capacity of cells expanded in FBS and HPL, with HPL supplementation resulting in almost three times more mineralized tissue within calcium phosphate scaffolds. FBS-expanded cells resulted in a fibrous tissue structure, whereas HPL resulted in mineralized tissue formation, which can be classified as newly formed bone, verified by μ CT and histological analysis. We also observed the presence of blood vessels in our explants. In conclusion, we suggest that replacing FBS with HPL in bioreactor-based expansion of hPDCs is an optimal solution that increases expansion efficiency along with promoting bone forming capacity of these cells. STEM CELLS TRANSLATIONAL MEDICINE 2019;8:810–821

SIGNIFICANCE STATEMENT

Current research in the field of stem cell bioprocessing has highlighted the need for xenogenic-free media and that will enhance process efficiency while facilitating clinical translation. This work provides important data and support toward the use of platelet lysate as a viable alternative to fetal bovine serum in a scalable suspension cell culture setup. Although human platelet lysate is increasingly considered for several progenitor cell types as a suitable medium for culture, there are no studies evaluating these cells in an in vivo setting. In this study, strikingly, hPDCs were seen to be able to form significantly higher amount of bone when implanted together with CaP carriers in small animal models. This capacity was linked to activation of WNT and BMP pathways associated with the osteogenic capacity of several progenitor cells.

INTRODUCTION

The fields of cell-based therapy, tissue engineering, and regenerative medicine aim to address unmet clinical challenges by using stem/progenitor cells as main therapeutic substances. Multipotent adult progenitors (encountered in multiple sources in the human body) are

especially attractive due to their relatively easy availability and better safety profile in comparison to pluripotent stem cells. This is highlighted by the fact that as of April 2018, there are over 850 registered clinical trials using MSCs (MSCs at ClinicalTrials.gov), in comparison to the approximate 500 trials registered in June 2015 [1]. From these, 26 studies are focused on bone

fracture healing and 11 for nonunions. It is estimated that for preclinical investigations using large animal models and clinical trials, the required number of progenitor cells could go up to millions per treatment. For example, it has been reported that between 15 and 45 million MSCs may be required for cartilage regeneration in joint surface defects and the number can go up to 600 million for a tibia defect of 4 cm [1–3]. Hence, the development of scalable and automated bioprocesses that could contribute to cost-efficient production of cell-based therapeutics, compliant with Good Manufacturing Practices, is necessary.

The efficiency of bioreactor-based processes is dependent on various extrinsic culture parameters. A key process parameter for such manufacturing processes is the culture medium and its composition. Traditionally, culture media used for most mammalian cells included fetal bovine serum (FBS) as a supplement. However, FBS possesses certain drawbacks, such as high lot-to-lot variation, potential for pathogen transfer, xenogeneic contaminations, and even limited supply. To address these issues, a shift toward alternate supplements and chemically defined media (CDM) has been advocated and intensively investigated. Human platelet lysate (HPL) has been suggested as an alternative option for FBS in recent years. It contains various growth factors like Transforming growth factor- β , Platelet derived growth factor, Insulin-like growth factor-1, bFGF, Epidermal growth factor, and Vascular endothelial growth factor along with adhesive proteins like fibrinogen and fibronectin [4, 5]. Similar to FBS, HPL also can have lot-to-lot variation due to its human origin. However, the large batch production method of commercially available HPL reduces the effect of such variation. The use of large number of donors (20–120 donors) also aids in decreasing lot-to-lot variations [6]. Extensive work has been carried out in two-dimensional (2D) static culture to investigate the use of HPL as an alternative to FBS for culture of MSCs from different sources including bone marrow (BM), umbilical cord blood (UCB), adipose tissue, and corneal stroma [7–12]. It was consistently reported that HPL supplementation resulted in enhanced cell proliferation in comparison to FBS. For example, the population doubling time for BM MSCs (between P1 and P2) in 10% FBS was reported to be approximately 20 days in comparison to 6 days for 10% HPL [7]. Schallmoser et al. and Capelli et al. also reported the feasibility of clinical scale expansion of MSCs from BM aspirate without any prior manipulation using HPL [8, 13]. It has also been reported that use of HPL enhances osteogenic and chondrogenic differentiation capabilities of MSCs in vitro [14–17].

With success in static cultures, HPL has also been used for expansion of MSCs within bioreactor setups. The earliest reported study for HPL-based MSC expansion in a bioreactor system was carried out by Petry et al. in 2015 wherein UCB MSCs were expanded using 10% HPL supplemented medium, on microcarriers in spinner flasks [18]. Heathman et al. also [19] demonstrated in 2016 that the use of HPL in microcarrier-based spinner flask culture of BM MSCs resulted in a smaller lag phase and increased yield in comparison to FBS. They further showed that the use of HPL increased interdonor consistency contributing to robust bioprocess outcomes and hence aiding the use of MSCs in clinical settings. In the same year, it was also reported that HPL supplemented medium could be used to isolate UCB MSCs and subsequently expand them

using spinner flasks [20]. Since the publication of these pioneering works, multiple studies have been carried out to expand MSCs from various sources using HPL supplementation in different bioreactor systems like stirred reactors of different volumes (100 ml to 50 l) [21–23] and hollow fiber systems [24–26].

Human periosteum-derived stem cells (hPDCs) have shown to play a key role in fracture healing via the formation of a transient fibrocartilaginous callus that is subsequently mineralized and replaced de novo by bone via endochondral ossification [27–29]. It has also been reported that in fracture healing, growth factors such as bone morphogenetic proteins (BMP) and β -catenin/wingless-related factors (WNT) are released from cells at the fracture site to recruit and trigger skeletal progenitor cells in the periosteum to aid the healing process. Hence, activation of BMP and WNT signaling is an important indicator of cell bone forming capacity [30]. There is an increasing research activity on their use as a cell's source for the production of skeletal Advanced Therapy Medicinal Products (ATMPs). From a biopsy of 1 g periosteum, it can roughly be estimated that 150,000 skeletal progenitor cells (plastic adhesive) can be isolated for further in vitro expansion. This low initial cell number renders efficient expansion processes crucial for the successful implementation of hPDC-based ATMPs. Under serum containing conditions, hPDCs have shown in vitro expansion potential for up to 30 population doublings exhibiting a fibroblast-like morphology and a population doubling time of 55 hours [2]. PDCs after ex vivo expansion have shown to have characteristics similar to MSCs derived from other sources [30–33]. Additionally, they have shown to possess superior bone forming properties to BM-derived and other MSC types when implanted subcutaneously on calcium phosphate (CaP) carriers [34, 35]. In previous studies, we have expanded hPDCs in various types of bioreactor including spinner flasks [2, 36–38]. Furthermore, when cultured in perfusion bioreactors in osteoinductive medium, hPDCs have shown to be able to differentiate into the osteogenic lineage producing mineralized extracellular matrix [39, 40], whereas in a spinner flask system, they were capable of undergoing chondrogenic differentiation [36].

Various studies have highlighted the positive effect of HPL on osteogenic differentiation of MSCs in vitro in 2D as well as in three-dimensional scaffold-based culture [16, 17, 41]. However, only one study to date has shown in vivo bone forming capacity of statically cultured BM-MSCs in HPL supplemented medium [42]. To the best of authors' knowledge, there is no reported study on the in vivo bone forming capacity of adult MSC populations expanded in bioreactors in HPL supplemented medium. In this work, the use of HPL for microcarrier-based expansion of hPDCs in spinner flasks was investigated in comparison to FBS supplementation. Differences in gene expression signature regarding MSC-markers (cluster of differentiation [CD]73, CD90, CD105), chondrogenic differentiation (SOX9, aggrecan [ACAN], collagen II [COL II], COLX), and osteogenic differentiation (RUNX2, collagen I [COL I], Osteocalcin [OCN], alkaline phosphatase [ALP], BMP2, WNT5) were investigated [30, 43]. Subsequently, the in vivo bone forming capacity of the expanded cell populations was evaluated using an ectopic model.

MATERIALS AND METHODS

hPDCs Static Culture

Human PDCs were obtained from periosteal biopsies with informed consent from the patient and approval of the Ethics

Committee for Human Medical Research (KU Leuven). Pooled hPDCs from four individual donors were expanded and maintained in high glucose containing Dulbecco's Modified Eagle's medium (DMEM, Invitrogen, Belgium) supplemented with 10% FBS (Hyclone, U.K.), 1% sodium pyruvate (Invitrogen), and 1% antibiotic-antimycotic (Invitrogen). Cells were incubated in a humidified incubator at 37°C with 5% CO₂. They were monitored regularly and on reaching a confluence of 90%, were detached with Tryple E (Invitrogen) and used for further experiments.

Spinner Flask Culture

One-hundred-milliliter spinner flasks with paddle-based impeller from Bellco Biotechnology (Bellco Glass, Inc., VWR International, Belgium) were used with a final volume of 80 ml. Coating of the flasks with SigmaCote (Sigma-Aldrich, St. Louis, MO) was carried out prior to usage. Cultispher S microcarriers (GE Healthcare, Belgium) at a concentration of 1 mg/ml were weighed, hydrated using phosphate-buffered saline (PBS), and sterilized by autoclaving. Twenty-four hours prior to the seeding of spinner flasks, T-flask expanded cells were put through a serum starvation process. Briefly, regular culture medium was removed from the flasks followed by PBS washes to remove all media traces. Complete medium containing 0.1% FBS was added to the flasks and incubated overnight. The low serum-based medium was removed, cells were washed with PBS, followed by seeding in spinner flasks with appropriate complete medium (either with 10% FBS or with 10% HPL [Stemulate, Cook Regentec, U.K.]). The microcarriers were also equilibrated prior to use by incubating them in culture medium overnight. A seeding density of 2.5×10^4 cells per milliliter along with attachment and expansion protocols in spinner flasks were selected based on previous publication [36]. hPDCs were expanded for 10 days in the spinner flask with 50% medium replacement every third day. Ten percentage HPL-based medium was selected based on preliminary static culture comparison (data not shown) and was compared with established 10% FBS supplementation. At specific time points throughout the experiment, cells and media were stored for analyses.

Cell Count and DNA Quantification

Cell viability and growth were estimated by DNA quantification and Trypan blue-based cell count. Cultispher S microcarriers were dissolved using collagenase type IV (Life Technologies, Belgium) in order to harvest the cells. For DNA quantification, cells were collected in lysis buffer (Qiagen, The Netherlands) and supplemented with β -mercaptoethanol followed by 30 seconds vortexing. Qubit dsDNA HS assay kit (Molecular Probes, Thermo Scientific, Belgium) was used for DNA measurement following manufacturer's protocol using Qubit Fluorometer (Invitrogen).

Medium Analysis

Metabolites were measured using Cedex Bio Analyzer (Roche Custom Biotech, Belgium). The media supernatant were collected and analyzed. Ammonia concentration was normalized with respect to its production in cell-free setup due to glutamine degradation. Specific metabolite consumption/production rate were calculated using Equation 1 [36].

$$q_{met} = \frac{C_{met(t)} - C_{met(t-1)}}{X \times t} \quad (1)$$

where q_{met} = cell-specific metabolite consumption/production rate; $C_{met(t)}$ = concentration of metabolite measured at the end of time point t ; $C_{met(t-1)}$ = concentration of metabolite at the start; and X = cell number at time t (day).

Live-Dead Assay

Live/Dead kit from Molecular Probes, Thermo Scientific was used to qualitatively analyze live and dead cells. Briefly, cell samples were taken from the spinner flask and washed twice with PBS. 0.5 μ l of Calcein-AM (4 mM stock) and 2 μ l of Ethidium Homodimer (2 mM stock) was added to 1 ml of PBS. One hundred microliters of the solution was added to the samples and incubated at 37°C for 30 minutes, followed by washing in PBS twice. They were then observed under fluorescence microscope (Discovery V8, Zeiss, Oberkochen, Germany).

DAPI, Phalloidin Staining

Cells on microcarriers were collected from the spinner flask for actin filament and nucleus staining. The cells were fixed using 4% paraformaldehyde (PFA) followed by incubation in 0.1 M glycine solution for 15 minutes. Cells were incubated for 20 minutes at room temperature in staining solution containing 2.5 μ l of DAPI (1 mg/ml stock solution), 4 μ l of phalloidin (200 U/ml stock concentration Alexa Fluor 488, phalloidin, Life Technologies), and 20 μ l of Triton-X per ml of PBS followed by imaging using confocal microscope (Zeiss, Oberkochen, Germany).

RNA Extraction, cDNA Synthesis, and qPCR Analysis

Total RNA was extracted using RNeasy mini kit (Qiagen) and was quantified using NanoDrop ND-1000 spectrophotometer (Thermo Scientific, Belgium). cDNA was synthesized using RevertAid H Minus first strand cDNA synthesis kit (Thermo Scientific, Belgium) for 500 ng of RNA. cDNA was stored at -20°C at a final concentration of 3.33 ng/ μ l. qPCR was carried out using SyBR Green Mastermix (ThermoFisher Scientific, Waltham, MA). The PCR cycle used was -45°C for 2 minutes, 95°C for 30 seconds, 40 cycles of 95°C for 3 seconds, and 60°C for 20 seconds. Each sample was tested in duplicate and compared with β -actin expression that allowed normalization of results. Relative differences in expression were calculated using the $2^{-\Delta\Delta\text{CT}}$ method.

MSC Phenotyping

Harvested cells were assessed based on a combined positivity for typical MSC CD markers and lack of expression for hematopoietic markers [36]. The used antibody panel was CD90-FITC, CD73-APC, CD105-PE, CD14, CD20, CD34, and CD45-PerCP (Miltenyi Biotec, Gladbach, Germany). Dead cells were excluded based on a viability dye. Flow cytometric analysis was carried out using BD FACS Canto. Automatic single-color compensation was performed by the acquisition software (BD FACSDiva, Franklin lakes, NJ) using compensation beads (UltraComp eBeads Affymetrix eBioscience, St Louis, MO). The gating was based on Fluorescence Minus One controls.

Trilineage In Vitro Differentiation Potential Analysis

In order to assess the multipotency maintenance capability of the cells, their trilineage differentiation, that is, chondrogenic, osteogenic, and adipogenic differentiation capability in vitro was tested [36, 44].

Chondrogenic differentiation of the hPDCs was assessed in a micromass assay. Briefly, 2×10^5 cells were resuspended in 10 μ l of regular culture medium and seeded as micromasses. After 2 hours of incubation, 0.5 ml of standard culture medium was added. After overnight incubation, the medium was replaced by chondrogenic medium consisting of DMEM/F12 (Life Technologies), 2% FBS, 1% antibiotic–antimycotic, 1% ITS Premix (Corning, New York, NY), 100 nM dexamethasone (Sigma, Belgium), 10 M Y27632 (Axon Medchem, Groningen, NL), 50 g/ml ascorbic acid, 40 g/ml proline, and 10 ng/ml recombinant human transforming growth factor β -1 (Preprotech, U.K.). After 7 days of chondrogenic induction, micromasses were fixed in ice-cold methanol and stained at room temperature for 1 hour with a 0.1% Alcian blue solution in 0.1 M HCl at pH 1.2. Alcian blue was extracted using 6 M guanidine hydrochloride and absorbance was measured at 620 nm.

Osteogenic differentiation was assessed by seeding the cells at a density of 4,500 cells per cm^2 in 0.5 ml culture medium. After 48 hours, the medium was replaced by standard culture medium supplemented with 100 mM dexamethasone, 50 g/ml ascorbic acid, and 10 mM β -glycerolphosphate. After 21 days, cells were fixed prior to analysis in ice-cold methanol for 1 hour and afterward stained with a 2% alizarin red S solution in Baxter water. Ten percentage cetylpyridinium chloride was used for stain extraction and measured at 540 nm.

Adipogenic differentiation was investigated by seeding the cultured hPDCs at a density of 1×10^4 cells per cm^2 in 0.5 ml standard culture medium. After 24 hours, the medium was replaced by adipogenic medium consisting of α -MEM (Life Technologies) supplemented with 10% FBS, 1% antibiotic–antimycotic, 1 M dexamethasone, 10 g/ml human insulin (Sigma), 100 M indomethacin (Sigma), and 25 M 3-isobutyl-1-methylxanthine (Sigma). After approximately 14 days (fat globules seen), cells were fixed in 10% formaldehyde for 20 minutes, rinsed shortly with 60% isopropanol and stained with Oil Red O. Staining from fat globules was extracted using isopropanol and measured at 518 nm. Samples in standard culture medium were used as negative control for all cases.

Ectopic In Vivo Implantation and Analysis

After 10 days of expansion, cells from spinner flasks were harvested using collagenase and ectopically implanted on the back of nude mice for 8 weeks. 1×10^6 cells in a total volume of 30 μ l culture medium were seeded on clinical grade CaP scaffolds (NuOss, ACE Surgical Supply Co., Inc., Hannover, Germany). They were incubated overnight (37°C, 5% CO_2 , 95% RH) followed by ectopic implantation. Empty CaP scaffolds were implanted as control. After 8 weeks, the explants were retrieved, fixed overnight in 4% PFA, and preserved in PBS before scanning by x-ray computed tomography and histological analysis. All animal experiments and procedures were approved by the Animal Ethics Committee (KU Leuven).

The volume of newly formed mineralized tissue after 8 weeks of in vivo implantation was determined by nano-Computed Tomography (CT) performed on a Phoenix NanoTom M (GE Measurement and Control) system. The applied scan settings were 60 kV x-ray voltage, 170 mA current, 500 milliseconds exposure time, a frame averaging of 1 and image skip of 0 and with a 3 μ m voxel size. Images were reconstructed with Phoenix Datos x CT software (GE Measurement and Control). The quantification of the bone volume was based on a two-level

automatic Otsu segmentation algorithm. All image processing was performed in CTAn (Bruker micro-CT, Kontich, BE).

At the end of CT analysis, the scaffolds were decalcified using EDTA for approximately 4 weeks followed by paraffin embedding, sectioning (5 μ m), and subsequent histological analysis. Hematoxylin–eosin, Safranin O–Fast Green, and Masson's trichrome staining were carried out as per established protocols.

Statistical Analysis

All quantitative results were expressed as mean \pm SEM. One-way analysis of variance followed by Dunnett's multiple comparison test was performed using GraphPad Prism, version 6.00 for Windows (GraphPad Software, La Jolla, CA) in order to find statistical significance of the data. Statistical significance analysis was carried out by comparing the experimental setups with mainly day 0 (D0) control setups. Exceptions are mentioned within the Materials and Methods and Results sections. Differences among data were considered to be statistically significant if $p < .05$.

RESULTS

Viable Cell Count and DNA Quantification

Preliminary studies showed that cell expansion with HPL in spinner flasks reached a plateau after day 10, suggesting that confluence may have been reached already at this time point. Hence, we restricted our studies until day 10. Cell expansion in both HPL-based and FBS-based media was regularly monitored via trypan blue-based cell count and DNA quantification. Cell attachment and spreading on microcarriers were also visualized based on actin and nucleus staining. As observed in Figure 1A, 1B, hPDCs were able to attach, spread uniformly, and proliferate on Cultispher S in both FBS and HPL supplemented media. Due to the opaque nature of Cultispher S, very little information can be gathered regarding cell attachment and expansion from phase-contrast microscopy. However, Figure 1C, 1D highlights the heterogeneous nature of Cultispher S microcarriers. Figure 1D also shows that by day 7, HPL-based medium results in "bead bridging" and clumping in the system due to higher cell density in comparison to FBS supplemented system. Both viable cell count and DNA quantification showed a steady increase in both FBS and HPL supplemented media suggesting cell proliferation within the system (Fig. 2A, 2B). However, the cell number in HPL was significantly higher than the FBS-based system from day 4 onward (Fig. 2A). At the end of 10 days culture, HPL showed a 4-fold increase of 5.2 ± 0.61 in comparison to that of FBS which had a 2.7 ± 0.22 -fold expansion. A similar trend was also observed for DNA quantification from extracted cells.

Live–Dead Assay

Calcein–ethidium homodimer staining was carried out to qualitatively estimate cell viability and death. As shown in Figure 2C, 2D, staining for both systems shows that hPDCs were viable in spinner flasks with negligible cell death. Bead–bead adhesion and clump formation were observed in both setups, but more prominent in HPL supplemented medium.

Metabolite Analysis

Spent media collected at various time points were analyzed for measuring and quantifying metabolites like glucose

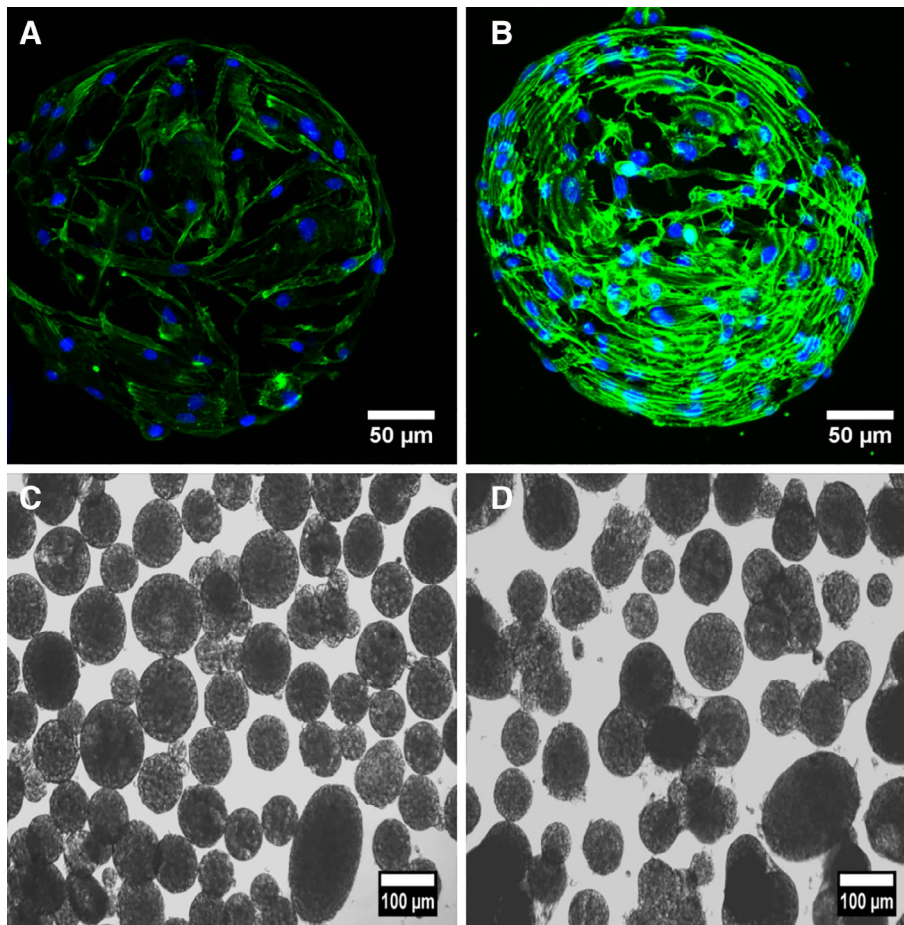


Figure 1. Visualization of human periosteum-derived cells attachment and expansion on Cultispher S for 10 days. **(A):** Nucleus-actin filament staining in fetal bovine serum (FBS) supplemented media on day 10, **(B)** nucleus-actin filament staining in human platelet lysate supplemented media on day 10, **(C)** phase-contrast image on day 7 for FBS supplemented media, **(D)** phase-contrast image on day 7 for human platelet lysate supplemented media. Scale bars: (A, B) = 50 μm ; (C, D) = 100 μm .

consumption, lactate production, Lactate Dehydrogenase (LDH) accumulation, and ammonia production. Glucose consumption rate (Fig. 3A) was significantly higher in HPL in comparison to FBS setup. The consumption showed a drop on day 10 for HPL containing cultures, suggesting a decrease in metabolic activity, which can be attributed to high-culture confluence or differentiation stage. Lactate production rate (Fig. 3B) and LDH production rate (Fig. 3E) increased over time and were higher in HPL supplemented medium in comparison to FBS, although a drop in their production rate can be seen on day 10 in both the systems. Lactate yield from glucose remained close to the theoretical value of 2 for HPL-based culture affirming that the system was metabolically active and robust. However, interestingly, the FBS system showed on days 4 and 7 a yield higher than the maximum theoretical value which decreased on day 10. Surprisingly, cumulative ammonia production rate showed opposite trends in the two systems. Within the FBS system, ammonia production showed a slight increase between day 4 and day 7, followed by a decrease on day 10. In contrast, HPL-based setup showed a sharp decrease in ammonia production between day 4 and day 7 followed by an increase on day 10. Overall, ammonia production was higher in FBS than in comparison to HPL culture with significant differences on days 7 and 10.

MSC Phenotyping

Based on flow cytometric analysis of spinner flask expanded cells, it was observed that for FBS supplementation, 89% of the cells showed simultaneously positive expression of CD73, CD90, and CD105 and negative expression for markers like CD14, CD20, CD34, and CD45 while the number was 86% for HPL supplemented setup (Fig. 4A). The individual marker expression at the protein level shows a slight drop in CD90 and CD73 expressing cell population (Fig. 4B).

In Vitro Trilineage Differentiation Capability

Trilineage differentiation capability of cells from spinner flask was measured and compared with control cells from T-flask. In vitro differentiation of cells toward chondrogenic, osteogenic, and adipogenic lineages were carried out (Fig. 5). Absorbance values of the different dyes after extraction were measured and compared with control data. No difference was observed for chondrogenic differentiation in both FBS and HPL supplemented media. Osteogenic differentiation capability was slightly upregulated in both HPL and FBS supplemented spinner flask culture in comparison to 2D control cultures. The upregulation was more for HPL in comparison to FBS.

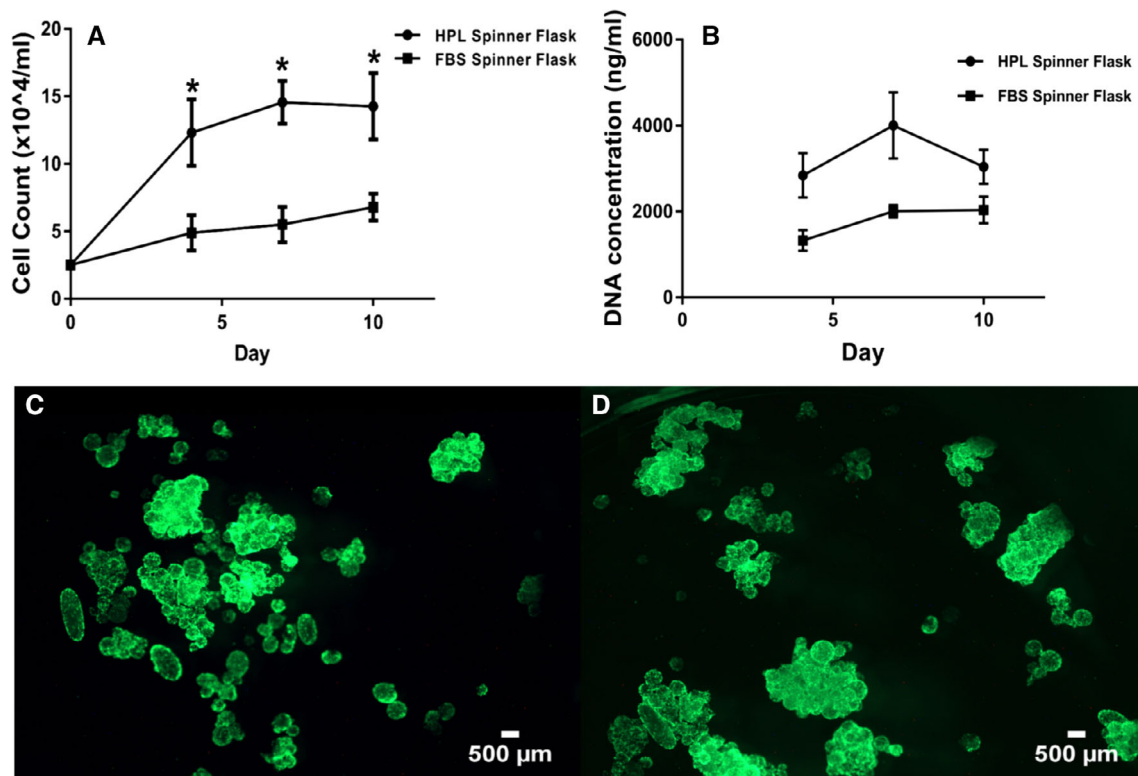


Figure 2. Quantification of cell expansion in fetal bovine serum (FBS) and human platelet lysate (HPL)-based spinner flask setup. **(A):** Trypan blue-based viable cell count, **(B)** DNA quantification of cell extracted from Cultispher S via collagenase treatment. **(C):** Live–dead qualitative analysis for FBS supplemented system on day 10, **(D)** live–dead qualitative analysis for HPL supplemented system on day 10. Merged images show cells on Cultispher S to be alive. Cell-microcarrier aggregation is also visible, suggesting confluence. Scale bar = 500 µm.

Interestingly, adipogenic differentiation capability for HPL supplemented system was significantly downregulated in comparison to the FBS supplemented setup.

mRNA Expression

qPCR-based analysis of mRNA expression was carried out for a host of markers for an in-depth analysis of the culture process at the end of 10-day culture period. Expression of the CD markers at the mRNA level (Fig. 6A) showed that CD73 was significantly downregulated in FBS in comparison to HPL supplemented culture. Both FBS-based and HPL-based systems showed a decrease on CD90 and CD105 expression in comparison to the D0 control cells. Sox9 expression in HPL supplemented setup was significantly higher in comparison to FBS whereas ACAN and COL II followed the reverse pattern (Fig. 6B). No significant difference was observed for Collagen X (COL X), RUNX2, and COL I. OCN was significantly upregulated for FBS in comparison to HPL whereas ALP had a significantly higher expression in HPL setup in comparison to FBS (Fig. 6C). Both BMP2 and WNT5A (Fig. 6D) were significantly upregulated in HPL in comparison to FBS. Adipogenic marker PPAR γ expression was lower in HPL-based system in comparison to FBS (Fig. 6E).

Micro-CT Analysis for In Vivo Bone Formation

Spinner flask expanded cells from both setups were ectopically implanted in nude mice using CaP scaffolds. After 8 weeks, the explants were analyzed for mineralized tissue content to assess bone forming capacity of FBS and HPL in spinner flask-based expansion. CT analysis showed a clear difference in

bone forming capacity between HPL-based and FBS-based system. As seen in Figure 7A, 7B, HPL showed mature mineralized tissue within the scaffold whereas use of FBS resulted in more fibrous tissue formation. Quantification of the mineralized tissue showed that HPL expansion resulted in a significantly higher volume of mineralized tissue in comparison to FBS-based spinner flask culture (Fig. 7C).

Histological Analysis

After μ -CT analysis, H&E, Safranin O-Fast Green, and Masson's trichrome staining were carried out for visualizing mineralization within the CaP scaffolds. As seen in Figure 7D–7O, histological staining supported μ -CT data. The FBS-based system mainly showed fibrous tissue structure within the scaffold with only very small fragments of bone tissue being formed. In contrast, the HPL-based system showed a much higher fully mineralized tissue which can be classified as “de novo bone” within the CaP scaffolds. Blood cell infiltration was also observed in both cases (Fig. 7E, 7G).

DISCUSSION

Efficient expansion of scarce autologous progenitor (MSC) populations is critical for clinical implementation and commercial viability of cell-based therapeutics [45]. Apart from their high proliferation rate in vitro and their multipotent nature, these cells also have lower regulatory and ethical complications than pluripotent cells, making their transition from bench

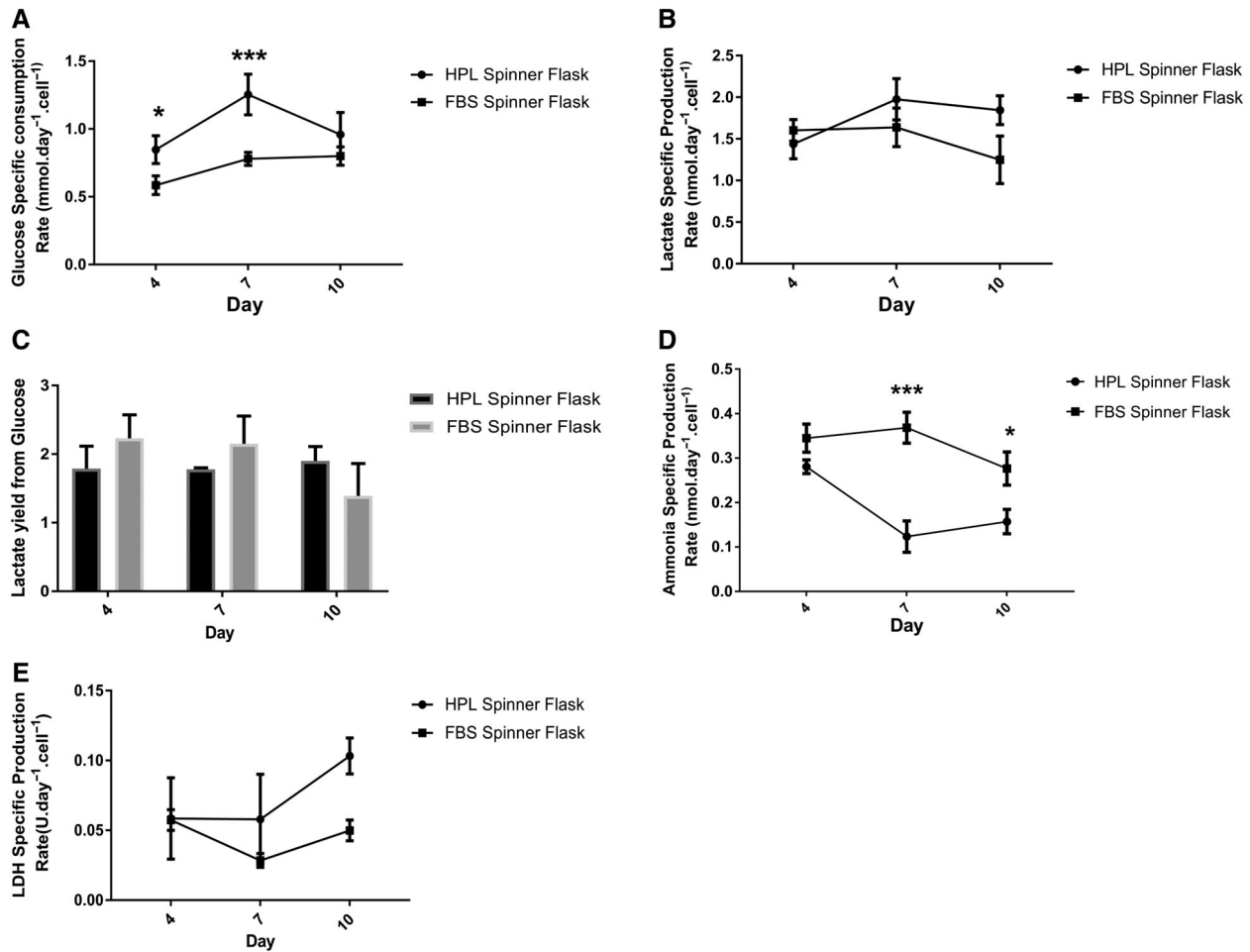


Figure 3. Metabolic analysis of spent media from spinner flask culture over 10 days. (A): Glucose-specific consumption rate, (B) lactate-specific production rate, (C) lactate yield from glucose, (D) ammonia-specific production rate, (E) LDH-specific production rate. ***, $p < .001$. One-way analysis of variance followed by Dunnett's multiple comparison test. Abbreviations: FBS, fetal bovine serum; HPL, human platelet lysate; LDH, lactate dehydrogenase.

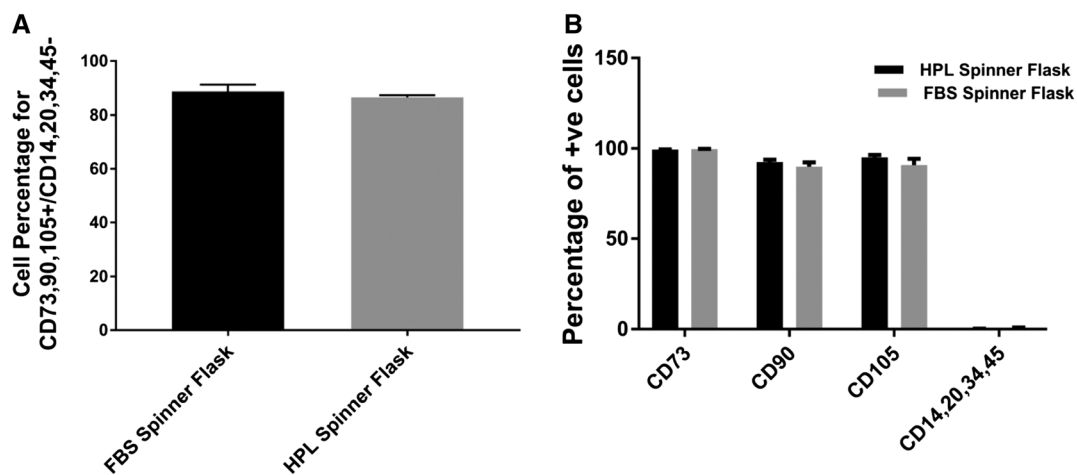


Figure 4. Mesenchymal stem cell (MSC) phenotypic markers expression. (A): Flow cytometric analysis for MSC marker combination expressing cells, and (B) expression of individual MSC phenotyping marker population.

to bedside relatively easier. hPDCs can be classified as MSCs originating from the periosteum, proven by their phenotypic characteristics [44]. However, methods for scaling up the

production of these cells are far from optimized to date. Efforts have been made to optimize upstream bioprocessing for MSCs using various bioreactor systems [46–48]. hPDCs

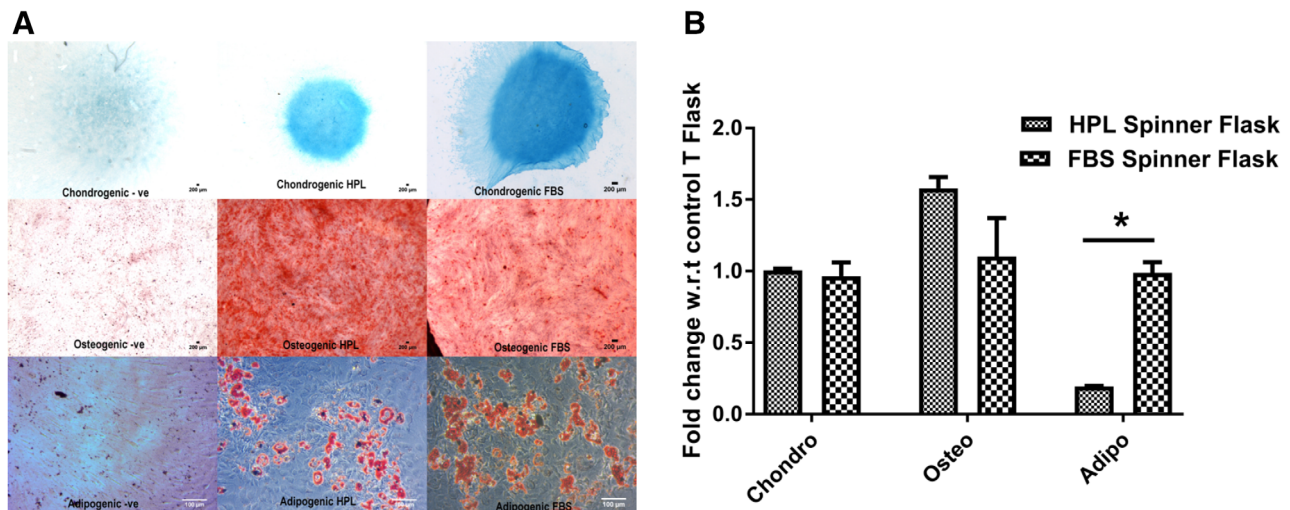


Figure 5. Analysis of trilineage differentiation capability of human periosteum-derived cells after 10 days of spinner flask culture, (A) qualitative analysis of Alcian blue, alizarin red, and Oil Red O staining for analyzing chondrogenic, osteogenic, and adipogenic differentiation potential, respectively. (B): Quantitative measurement of extracted dye from chondrogenic, osteogenic, and adipogenic differentiation. Fold change was calculated in comparison to differentiation of cells from T flask expansion in HPL and FBS as appropriate. Scale bar for chondrogenic and osteogenic = 500 μ m. Scale bar for adipogenic = 100 μ m. *, $p < .05$; one-way analysis of variance followed by Dunnett's multiple comparison test. Abbreviations: FBS, fetal bovine serum; HPL, human platelet lysate.

have been expanded and differentiated using hollow fiber, parallel plate, and stirred type bioreactors [2, 36–38, 40]. Spinner flasks or stirred reactors are one of the most attractive bioreactor setups due to their scalability and process flexibility. In this study, we explored FBS-based and HPL-based bioreactor process for scalable hPDC expansion. Apart from in vitro characterization, we evaluated the effects of HPL and FBS on the bone forming capacity of hPDCs in a nude mice model. Even though an increasing number of studies document the impact of HPL on various MSC populations, there are very few reports on the regenerative capacity of HPL-expanded cell populations upon implantation and none for in vivo bone forming potential.

The current work showed that supplementing expansion medium with HPL instead of FBS is beneficial for a microcarrier-based stirred process in terms of cell expansion, priming, and postexpansion bone forming capacity in the ectopic nude mice model. We observed and increased cell proliferation in HPL-based culture in comparison to FBS. Our data is supported by published proteomic analysis of HPL wherein analysis of extracellular cues from HPL showed involvement of pathways related to cell proliferation and wound repair [49]. Furthermore, glucose consumption rate for HPL-based system was significantly higher on days 4 and 7 in comparison to FBS with a drop toward the end of the expansion phase. For example, approximately 50% increase in glucose consumption rate was observed for HPL in comparison to FBS on day 7. Lactate production rate also showed a similar trend. Such a trend of lowered metabolic activity has been previously reported for MSCs from BM in spinner flask culture, although the timeline was different due to difference in cell origin, culture protocol, seeding density, and so on [50]. LDH production has been associated to cell death [51, 52] and also followed a pattern similar to lactate production. This can be linked to both, a higher starting LDH concentration in HPL in comparison to FBS, as well as faster cell growth and higher cell number present in the HPL containing medium. In contrast, ammonia production rate was different between the two systems with FBS-based system showing higher production

rate in comparison to HPL. Ammonia has been primarily known to be a by-product of glutamine degradation and consumption. The differing trend of its production in the two systems suggests that their glutamine catabolism is different. The lactate yield from glucose values for HPL-based system was very near to the theoretical value of 2 highlighting the metabolic robustness of the HPL-based process, which is important for MSC proliferation [53]. FBS supplementation, on the other hand, had a lactate yield from glucose value higher than 2 in the initial culture period. This has been reported before for MSCs in bioreactors and had been associated with the use of glutamine as an alternative carbon source by the cells [46]. The high ammonia production that we observed with FBS in the initial days of the culture further supports this theory. This further highlights the importance of metabolites and growth factor in the media along with their role in cell metabolism and merits further studies.

Flow cytometric analysis at the end of the culture period showed no discernible difference between the two systems in terms of MSC phenotypic markers. A significant difference was observed in the mRNA expression of CD73 wherein the HPL supplementation showed a higher expression in comparison to FBS. CD73 as an ecto 5' nucleotidase plays an important role in extracellular adenosine generation, although very little is known about their exact role in MSCs. It has been reported that CD73 is a regulator of osteo/chondrogenic differentiation via the adenosine receptor pathway with its downregulation supporting chondrogenesis in appropriate media [54, 55]. Others have also reported the importance of CD73 in the immunomodulatory/immunosuppressive effects shown by MSCs [56, 57]. However, this difference in CD73 expression was not observed at the protein level as evidenced by flow cytometry, hence the functional consequence is not known.

Considering HPL contains a wide variety of growth factors and that shear stress is a known factor in affecting cells' phenotypic state, we measured the expression of various differentiation related markers at the mRNA level, which highlighted interesting differences between FBS and HPL supplementation.

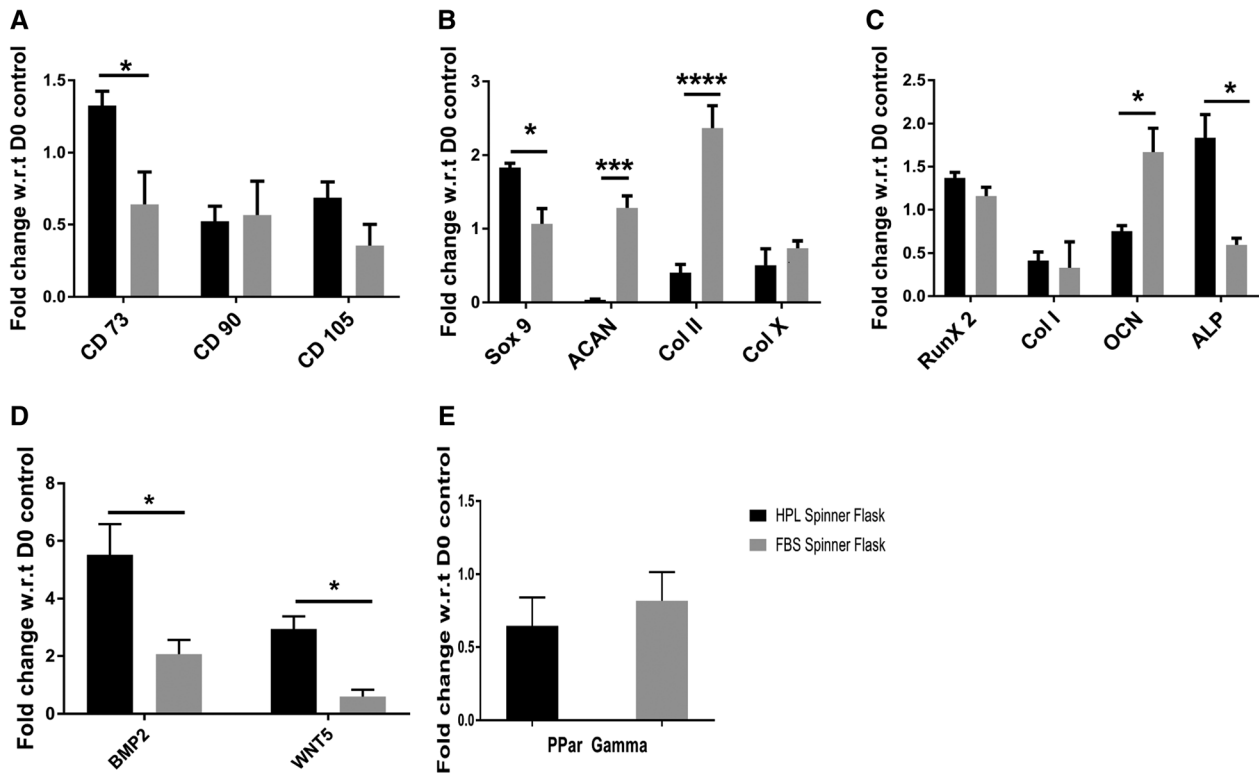


Figure 6. Quantitative analysis of mRNA expressions via qPCR for FBS and HPL supplemented spinner flasks at the end of 10 day culture period. **(A):** CD73, CD90, and CD105 expressions, **(B)** Sox9, ACAN, COL II, and COL X expressions. **(C):** RUNX2, COL I, OCN, and ALP expressions. **(D):** BMP2, WNT5A, **(E)** PPAR γ . *, $p < .05$; ***, $p < .001$; one-way analysis of variance followed by Dunnet's multiple comparison test. Abbreviations: ACAN, aggrecan; ALP, alkaline phosphatase; BMP2, bone morphogenetic protein-2; COL I, collagen I; FBS, fetal bovine serum; HPL, human platelet lysate; OCN, osteocalcin; WNT5A, wingless-related factor-5A.

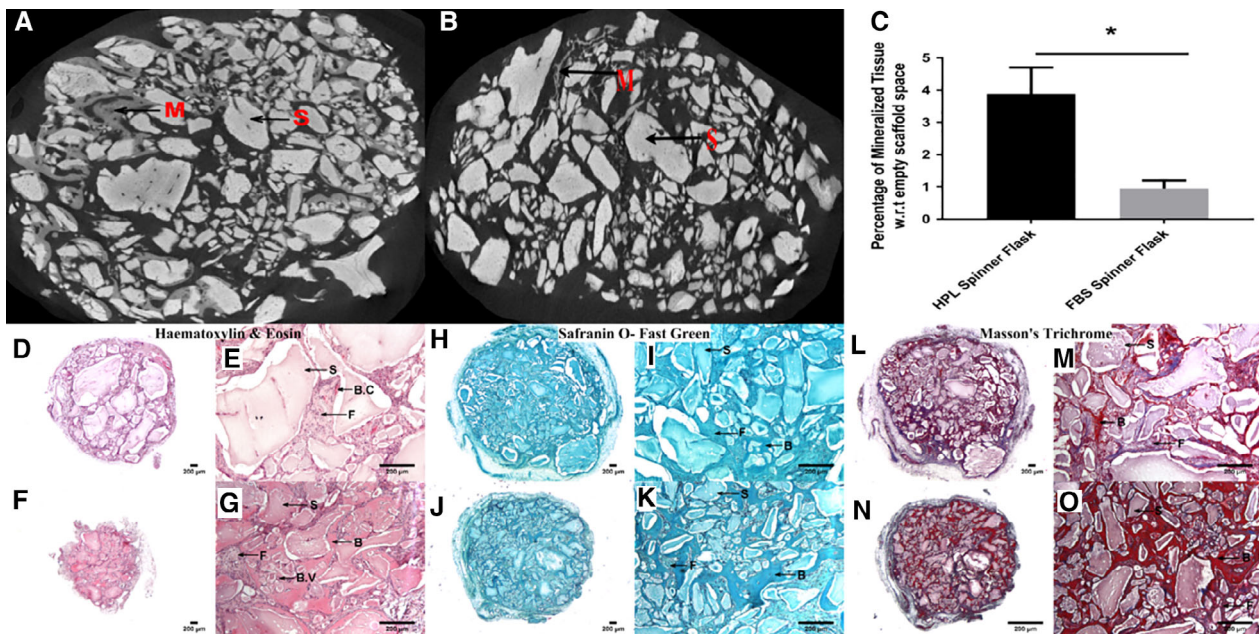


Figure 7. **(A):** Representative image of μ -CT analysis for estimating mineralized tissue within CaP scaffolds for HPL-based system. **(B):** representative image of μ -CT analysis for estimating mineralized tissue within CaP scaffolds for fetal bovine serum (FBS)-based system. **(C):** Quantification of mineralized tissue volume in CaP scaffolds for HPL and FBS-based spinner flask culture after 8 weeks of ectopic implantation. *, $p < .05$; one-way analysis of variance. **(D–O):** Histological analysis of 8 week nude mice explants of CaP scaffolds with human periosteum-derived cells grown in spinner flask using FBS and human platelet lysate (HPL)-based media. **(D, E):** H&E staining for HPL system explants, **(F, G)** H&E staining for FBS system explants, **(H, I)** Saf O-fast green staining for HPL system explants, **(J, K)** Saf O-fast green staining for FBS system explants, **(L, M)** Masson's trichrome staining for HPL system explants, **(N, O)** Masson's trichrome staining for FBS system explants. Abbreviations: B, de novo bone/mineralized tissue; B.C., blood cells; B.V., blood vessels; F, fibrous tissue; M, mineralized tissue; S, CaP scaffold particle; S, scaffold grain. Scale bar = 200 μ m.

The mRNA expression level of early osteochondrogenic transcription factor, SOX9 was significantly higher in HPL containing medium in comparison to FBS. Sox9 is considered to be a master regulator for chondrogenesis and is expressed in the early stages of differentiation [58] and also regulates expression of both ACAN and COL II at a later stage [59–62]. COL II and ACAN had significantly higher expression in FBS containing medium along with OCN. For example, COL II expression showed approximately 130% increase in HPL-based culture in comparison to FBS. RUNX2, which is also a marker for osteochondro progenitors had a higher expression in HPL-based system. The expression level of the hypertrophic (late chondrogenic) marker COL X remained low in both cases but was slightly higher in FBS in comparison to HPL. Taken together, these data may suggest that HPL maintain hPDCs at an earlier stage of differentiation in terms of chondrogenesis in comparison to FBS which might be pushing the hPDCs toward a more committed differentiation state. It could be also postulated that an osteochondral progenitor population could be preferentially expanded in HPL. In addition, the early osteogenic marker ALP was significantly higher in HPL than FBS [63]. Similar observations have been reported previously by Castrén et al. for 2D HPL and FBS culture [64]. They suggested that the differences in the temporal profile can be attributed to the presence of different growth factors in FBS and HPL.

In vitro trilineage differentiation capability of the hPDCs after spinner flask-based expansion was carried out as well. No discernible difference was seen between HPL and FBS supplementation on chondrogenic differentiation whereas osteogenic differentiation was nonsignificantly elevated in HPL. However, we noticed a significant drop in adipogenic differentiation capability of cells when expanded in HPL in comparison to FBS. This was highlighted further by a decreased mRNA expression level for PPAR γ in HPL containing system in comparison to FBS. This observation could also support the theory of preferential expansion of osteochondral progenitor subpopulations in HPL. Similar observations, that is, higher osteogenic and lower adipogenic differentiation potential of BM MSC in HPL-based medium has been reported previously [41, 65].

In order to assess the functionality of the expanded hPDCs, we harvested cells and implanted them ectopically in nude mice using CaP scaffolds using a robust in vivo assay developed previously [66]. μ -CT analysis showed that cells expanded in HPL formed mature mineralized tissue within the CaP scaffolds whereas FBS-expanded cells exhibited a more fibrous morphology. HPL supplementation also showed a significantly higher percentage of mineralization in comparison to FBS. This was clearly supported by H&E as well as Safranin O-Fast Green staining whereas Masson's trichrome showed higher quantity of newly formed bone in the HPL-expanded hPDCs in contrast to the collagenous and fibrous tissue generated by the FBS-expanded cells. The increase in osteogenic potential of hPDCs in HPL, as seen in the in vitro trilineage differentiation assay, appeared to be a prelude to the in vivo observations. In an effort to elucidate the reason behind this difference in ectopic bone formation capacity, we evaluated mRNA expression levels of BMP2 and WNT5A, two key players in MSC osteogenic differentiation pathways [43]. qPCR analysis showed that both BMP2 and WNT5A expression were significantly higher in HPL-based system in comparison to FBS at the end of spinner flask expansion. It has been previously reported that in vivo bone formation by hPDCs on CaP scaffolds

is promoted by upregulation of BMP and WNT pathways and that early expression of BMP and WNT promoted osteogenesis [30]. This report further supports our hypothesis that the observed high expression of BMP2 and WNT5A in HPL supplemented system primes the hPDCs toward improved bone formation in vivo. WNT5A has also been reported to be a repressor of PPAR γ expression [67] which is in sync with our observations of high WNT5A expression, lower PPAR γ expression, and lower adipogenic potential of hPDCs expanded in HPL. Both BMP2 and WNT5A specifically have also been reported to promote MSC osteogenesis [68–71]. The high expression level of these two markers in our HPL supplemented culture may partially explain the marked difference in in vivo bone formation as observed in the nude mice model. In addition, a recent publication has reported a global phenotypic analysis of surface markers for MSCs cultured in FBS and HPL. Importantly, it was reported that differential expression on multiple markers in HPL-expanded cells was specifically related to pathways involved in proliferation, osteogenic differentiation, and inflammatory responses [72]. This further supports our observation of increased proliferation and higher in vivo bone formatting capacity of hPDCs expanded in spinner flasks using HPL supplemented medium.

CONCLUSION

Our current work and published data from various other groups highlight the benefits of HPL in MSC expansion and differentiation. However, due to its origin, it has to be kept in mind that HPL may also have lot-to-lot variation and requires basic checks and preliminary studies on changing its procurement source and method. Performing similar studies with different batches of HPL may provide additional robustness to the data. Additionally, evaluating HPL expansion on hPDCs, freshly isolated from periosteal biopsies and then serially expanded until clinically relevant cell populations are reached, remains to be studied. In addition to the use of HPL, CDM can substitute the use of serum in cell culture along with minimizing problems arising due to batch-to-batch variation. Different groups have studied the feasibility of using serum free CDM for the expansion of MSCs in 2D as well as in microcarrier-based expansion in spinner flasks. It was demonstrated that in 2D culture, growth of MSCs in CDM was similar to serum-based medium, whereas donor-dependent variation was decreased on using CDM [73, 74]. However, it was reported that cell attachment and growth on microcarriers was slower on using CDM in comparison to FBS-based setup. This was attributed to the lack of various growth factors which are integral within a serum-based medium [75]. We demonstrated that replacing FBS with HPL as culture medium for spinner flask-based expansion of hPDCs on collagen microcarriers had multiple positive effects. These included a dramatic increase in cell proliferation and at the same time a significant improvement in bone forming capacity of expanded hPDCs, which is of utmost importance to autologous manufacture. In addition, the faster proliferation of MSCs in HPL, is expected to decrease the overall culture period significantly which in turn is expected to make the use of HPL more cost-effective in the long run. Evidence for functionality of expanded progenitor populations is often omitted from studies investigating HPL as an alternative expansion medium; thus, we believe that this study addresses an important question in the field of

cell therapy bioprocessing. These observations render the use of HPL for bone tissue engineering a suitable strategy resulting in bioprocesses of higher efficiency with the potential of improved clinical outcomes.

ACKNOWLEDGMENTS

F.P.L. and I.P. share senior authorship. This work is a part of Prometheus, the Leuven R&D Division of Skeletal Tissue Engineering. The funders had no role in study design, data collection and analysis, decision to publish, or preparation of the article. P.G. was funded by an advanced ERC grant (FP/2007–2013/ERC grant agreement number 294191). I.P. and G.N.H. were funded by FWO fellowship (project 1207916N and 1S05116N). We thank Kathleen Bosmans and Carla Geeroms for their assistance with *in vivo* implantation and CT analysis, respectively. The CT analysis was financed by the Hercules Foundation (project AKUL/13/47). Confocal images were recorded on a Zeiss LSM 780—SP Mai Tai HP DS (Cell and Tissue Imaging Cluster,

supported by Hercules AKUL/11/37 and FWO G.0929.15 to Pieter Vanden Berghe). P.G. is currently affiliated with the Department of Chemical and Process Engineering, University of Surrey, Guildford, United Kingdom.

AUTHOR CONTRIBUTIONS

P.G.: conception and design of experiments, data collection, data analysis and interpretation, manuscript writing; G.N.H.: data collection and reviewing of manuscript; L.G.: manuscript reviewing, conception and design of experiments, data interpretation; I.P.: manuscript writing and reviewing, conception and design of experiments, data interpretation; F.P.L.: financial assistance, manuscript reviewing.

DISCLOSURE OF POTENTIAL CONFLICTS OF INTEREST

The authors indicated no potential conflicts of interest.

REFERENCES

- Tan KY, Reuveny S, Oh SKW. Recent advances in serum-free microcarrier expansion of mesenchymal stromal cells: Parameters to be optimized. *Biochem Biophys Res Commun* 2016;473:769–773.
- Lambrechts T, Papantonou I, Rice B et al. Large-scale progenitor cell expansion for multiple donors in a monitored hollow fibre bioreactor. *Cytotherapy* 2016;18:1219–1233.
- Wakitani S, Imoto K, Yamamoto T et al. Human autologous culture expanded bone marrow mesenchymal cell transplantation for repair of cartilage defects in osteoarthritic knees. *Osteoarthr Cartil* 2002;10:199–206.
- Doucet C, Ernou I, Zhang Y et al. Platelet lysates promote mesenchymal stem cell expansion: A safety substitute for animal serum in cell-based therapy applications. *J Cell Physiol* 2005;205:228–236.
- Müller AM, Davenport M, Verrier S et al. Platelet lysate as a serum substitute for 2D static and 3D perfusion culture of stromal vascular fraction cells from human adipose tissue. *Tissue Eng Part A* 2009;15:869–875.
- Strunk D, Lozano M, Marks D et al. International forum on Gmp-grade human platelet lysate for cell propagation: Summary. *Vox Sang* 2018;113:80–87.
- Azouna NB, Jenhani F, Regaya Z et al. Phenotypical and functional characteristics of mesenchymal stem cells from bone marrow: Comparison of culture using different media supplemented with human platelet lysate or fetal bovine serum. *Stem Cell Res Ther* 2012;3:6.
- Capelli C, Domenghini M, Borleri G et al. Human platelet lysate allows expansion and clinical grade production of mesenchymal stromal cells from small samples of bone marrow aspirates or marrow filter washouts. *Bone Marrow Transplant* 2007;40:785–791.
- Fazzina R, Iudicone P, Fioravanti D et al. Potency testing of mesenchymal stromal cell growth expanded in human platelet lysate from different human tissues. *Stem Cell Res Ther* 2016;7:122.
- Lange C, Kakiroglu F, Spiess AN et al. Accelerated and safe expansion of human mesenchymal stromal cells in animal serum-free medium for transplantation and regenerative medicine. *J Cell Physiol* 2007;213:18–26.
- Matthysen S, Dhubhghail SN, Van Gerwen V et al. Xeno-free cultivation of mesenchymal stem cells from the corneal stroma. *Invest Ophthalmol Vis Sci* 2017;58:2659–2665.
- Reinisch A, Bartmann C, Rohde E et al. Humanized system to propagate cord blood-derived multipotent mesenchymal stromal cells for clinical application. *Regen Med* 2007;2:371–382.
- Schallmoser K, Rohde E, Reinisch A et al. Rapid large-scale expansion of functional mesenchymal stem cells from unmanipulated bone marrow without animal serum. *Tissue Eng Part C Methods* 2008;14:185–196.
- Galeano-Garces C, Camilleri ET, Riester SM et al. Molecular validation of chondrogenic differentiation and hypoxia responsiveness of platelet-lysate expanded adipose tissue-derived human mesenchymal stromal cells. *Cartilage* 2017;8:283–299.
- Hassan G, Bahjat M, Kasem I et al. Platelet lysate induces chondrogenic differentiation of umbilical cord-derived mesenchymal stem cells. *Cell Mol Biol Lett* 2018;23:11.
- Jonsdottir-Buch SM, Lieder R, Sigurjonsson OE. Platelet lysates produced from expired platelet concentrates support growth and osteogenic differentiation of mesenchymal stem cells. *PLoS One* 2013;8:e68984.
- Salvade A, Mina PD, Gaddi D et al. Characterization of platelet lysate cultured mesenchymal stromal cells and their potential use in tissue-engineered osteogenic devices for the treatment of bone defects. *Tissue Eng Part C Methods* 2009;16:201–214.
- Petry F, Smith JR, Leber J et al. Manufacturing of human umbilical cord mesenchymal stromal cells on microcarriers in a dynamic system for clinical use. *Stem Cells Int* 2016;2016:1–12.
- Heathman TR, Stolzing A, Fabian C et al. Scalability and process transfer of mesenchymal stromal cell production from monolayer to microcarrier culture using human platelet lysate. *Cytotherapy* 2016;18:523–535.
- Soure AM, Fernandes-Platzgummer A, Moreira F et al. Integrated culture platform based on a human platelet lysate supplement for the isolation and scalable manufacturing of umbilical cord matrix-derived mesenchymal stem/stromal cells. *J Tissue Eng Regen Med* 2017;11:1630–1640.
- Gadelorge M, Bourdens M, Espagnolle N et al. Clinical-scale expansion of adipose-derived stromal cells starting from stromal vascular fraction in a single-use bioreactor: Proof of concept for autologous applications. *J Tissue Eng Regen Med* 2018;12:129–141.
- Lawson T, Kehoe DE, Schnitzler AC et al. Process development for expansion of human mesenchymal stromal cells in a 50L single-use stirred tank bioreactor. *Biochem Eng J* 2017;120:49–62.
- Rafiq QA, Ruck S, Hanga MP et al. Qualitative and quantitative demonstration of bead-to-bead transfer with bone marrow-derived human mesenchymal stem cells on microcarriers: Utilising the phenomenon to improve culture performance. *Biochem Eng J* 2018;135:11–21.
- Bellio MA, Khan A. 74—Expanding mesenchymal stem cells with platelet lysate vs FBS increases bioreactor efficiency but alters cytokine profile. *Cytotherapy* 2018;20:S29.
- Haack-Sørensen M, Juhl M, Follin B et al. Development of large-scale manufacturing of adipose-derived stromal cells for clinical applications using bioreactors and human platelet lysate. *Scand J Clin Lab Invest* 2018;78:1–8.
- Mizukami A, de Abreu Neto MS, Moreira F et al. A fully-closed and automated hollow fiber bioreactor for clinical-grade manufacturing of human mesenchymal stem/stromal cells. *Stem Cell Rev* 2018;14:141–143.
- Colnot C. Skeletal cell fate decisions within periosteum and bone marrow during bone regeneration. *J Bone Miner Res* 2009;24:274–282.

- 28 De Lageneste OD, Julien A, Abou-Khalil R et al. Periosteum contains skeletal stem cells with high bone regenerative potential controlled by Periostin. 2018;9:773.
- 29 Zhang X, Awad HA, O'Keefe RJ et al. A perspective: Engineering periosteum for structural bone graft healing. *Clin Orthop Relat Res* 2008;466:1777–1787.
- 30 Bolander J, Chai YC, Geris L et al. Early BMP, Wnt and Ca²⁺/PKC pathway activation predicts the bone forming capacity of periosteal cells in combination with calcium phosphates. 2016;86:106–118.
- 31 De Bari C, Dell'Accio F, Luyten FP. Human periosteum-derived cells maintain phenotypic stability and chondrogenic potential throughout expansion regardless of donor age. *Arthritis Rheumatol* 2001;44:85–95.
- 32 Bolander J, Ji W, Leijten J et al. Healing of a large long-bone defect through serum-free in vitro priming of human periosteum-derived cells. 2017;8:758–772.
- 33 Eyckmans J, Roberts SJ, Bolander J et al. Mapping calcium phosphate activated gene networks as a strategy for targeted osteoinduction of human progenitors. 2013;34:4612–4621.
- 34 Bolander J, Ji W, Geris L et al. The combined mechanism of bone morphogenetic protein-and calcium phosphate-induced skeletal tissue formation by human periosteum derived cells. 2016;30:11–25.
- 35 Roberts SJ, van Gastel N, Carmeliet G et al. Uncovering the periosteum for skeletal regeneration: The stem cell that lies beneath. *Bone* 2015;70:10–18.
- 36 Gupta P, Geris L, Luyten FP et al. An integrated bioprocess for the expansion and chondrogenic priming of human periosteum-derived progenitor cells in suspension bioreactors. *Biotechnol J* 2018;13. <https://doi.org/10.1002/biot.201700087>.
- 37 Lambrechts T, Papantoniou I, Viazzi S et al. Evaluation of a monitored multiplate bioreactor for large-scale expansion of human periosteum derived stem cells for bone tissue engineering applications. *Biochem Eng J* 2016;108:58–68.
- 38 Sonnaert M, Papantoniou I, Bloemen V et al. Human periosteal-derived cell expansion in a perfusion bioreactor system: Proliferation, differentiation and extracellular matrix formation. *J Tissue Eng Regen Med* 2017;11:519–530.
- 39 Papantoniou I, Guyot Y, Sonnaert M et al. Spatial optimization in perfusion bioreactors improves bone tissue-engineered construct quality attributes. *Biotechnol Bioeng* 2014;111:2560–2570.
- 40 Papantoniou I, Sonnaert M, Lambrechts T et al. Analysis of gene expression signatures for osteogenic 3D perfusion-bioreactor cell cultures based on a multifactorial DoE approach. *Processes* 2014;2:639–657.
- 41 Xia W, Li H, Wang Z et al. Human platelet lysate supports ex vivo expansion and enhances osteogenic differentiation of human bone marrow-derived mesenchymal stem cells. *Cell Biol Int* 2011;35:639–643.
- 42 Chevallier N, Anagnostou F, Zilber S et al. Osteoblastic differentiation of human mesenchymal stem cells with platelet lysate. *Biomaterials* 2010;31:270–278.
- 43 Nemoto E, Ebe Y, Kanaya S et al. Wnt5a signaling is a substantial constituent in bone morphogenetic protein-2-mediated osteoblastogenesis. 2012;422:627–632.
- 44 De Bari C, Dell'Accio F, Vanlauwe J et al. Mesenchymal multipotency of adult human periosteal cells demonstrated by single-cell lineage analysis. *Arthritis Rheum* 2006;54:1209–1221.
- 45 Papantoniou I, Lambrechts T, JMCGTI A. Bioprocess engineering strategies for autologous human MSC-based therapies: One size does not fit all. 2017;3:469–482.
- 46 Rafiq QA, Brosnan KM, Coopman K et al. Culture of human mesenchymal stem cells on microcarriers in a 5 l stirred-tank bioreactor. *Biotechnol Lett* 2013;35:1233–1245.
- 47 Rafiq QA, Coopman K, Nienow AW et al. Systematic microcarrier screening and agitated culture conditions improves human mesenchymal stem cell yield in bioreactors. *Biotechnol J* 2016;11:473–486.
- 48 Sart S, Schneider Y-J, Agathos SN. Influence of culture parameters on ear mesenchymal stem cells expanded on microcarriers. *J Biotechnol* 2010;150:149–160.
- 49 Crespo-Diaz R, Behfar A, Butler GW et al. Platelet lysate consisting of a natural repair proteome supports human mesenchymal stem cell proliferation and chromosomal stability. *Cell Transplant* 2011;20:797–812.
- 50 Santos F, Andrade PZ, Abecasis MM et al. Toward a clinical-grade expansion of mesenchymal stem cells from human sources: A microcarrier-based culture system under xeno-free conditions. 2011;17:1201–1210.
- 51 Legrand C, Bour J, Jacob C et al. Lactate dehydrogenase (LDH) activity of the number of dead cells in the medium of cultured eukaryotic cells as marker. 1992;25:231–243.
- 52 Wagner A, Marc A, Engasser J et al. The use of lactate dehydrogenase (LDH) release kinetics for the evaluation of death and growth of mammalian cells in perfusion reactors. 1992;39:320–326.
- 53 Sart S, Agathos SN, Li Y. Process engineering of stem cell metabolism for large scale expansion and differentiation in bioreactors. *Biochem Eng J* 2014;84:74–82.
- 54 Ode A, Kopf J, Kurtz A et al. CD73 and CD29 concurrently mediate the mechanically induced decrease of migratory capacity of mesenchymal stromal cells. *Eur Cell Mater* 2011;24:26–42.
- 55 Ode A, Schoon J, Kurtz A et al. CD73/5'-ecto-nucleotidase acts as a regulatory factor in osteo-/chondrogenic differentiation of mechanically stimulated mesenchymal stromal cells. *Eur Cell Mater* 2013;25:37–47.
- 56 Chen X, Shao H, Zhi Y et al. CD73 pathway contributes to the immunosuppressive ability of mesenchymal stem cells in intraocular autoimmune responses. 2016;25:337–346.
- 57 Kerkelä E, Laitinen A, Rabinä J et al. Adenosinergic immunosuppression by human mesenchymal stromal cells requires co-operation with T cells. *STEM CELLS* 2016;34:781–790.
- 58 Kawakami Y, Rodriguez-León J, Belmonte JCI. The role of TGFβs and Sox9 during limb chondrogenesis. *Curr Opin Cell Biol* 2006;18:723–729.
- 59 Bell DM, Leung KKH, Wheatley SC et al. SOX9 directly regulates the type-II collagen gene. *Nat Genet* 1997;16:174–178.
- 60 Han Y, Lefebvre V. L-Sox5 and Sox6 drive expression of the aggrecan gene in cartilage by securing binding of Sox9 to a far-upstream enhancer. *Mol Cell Biol* 2008;28:4999–5013.
- 61 Yasuda H, Oh C-D, Chen D et al. A novel regulatory mechanism of type II collagen expression via a SOX9-dependent enhancer in intron 6. *J Biol Chem* 2016;292:528–538. <https://doi.org/10.1074/jbc.M116.758425>.
- 62 Vega SL, Kwon MY, Song KH et al. Combinatorial hydrogels with biochemical gradients for screening 3D cellular microenvironments. 2018;9:614.
- 63 Aubin JEJRE, Disorders M. Regulation of osteoblast formation and function. *Rev Endocr Metab Disord* 2001;2:81–94.
- 64 Castrén E, Sillat T, Oja S et al. Osteogenic differentiation of mesenchymal stromal cells in two-dimensional and three-dimensional cultures without animal serum. *Stem Cell Res Ther* 2015;6:167.
- 65 Horn P, Bokermann G, Cholewa D et al. Impact of individual platelet lysates on isolation and growth of human mesenchymal stromal cells. *Cytotherapy* 2010;12:888–898.
- 66 Roberts SJ, Geris L, Kerckhofs G et al. The combined bone forming capacity of human periosteal derived cells and calcium phosphates. *Biomaterials* 2011;32:4393–4405.
- 67 Takada I, Kouzmenko AP, Kato S. Wnt and PPARγ signaling in osteoblastogenesis and adipogenesis. *Nat Rev Rheumatol* 2009;5:442–447.
- 68 Boland GM, Perkins G, Hall DJ et al. Wnt 3a promotes proliferation and suppresses osteogenic differentiation of adult human mesenchymal stem cells. *J Cell Biochem* 2004;93:1210–1230.
- 69 Chen Z, Wu C, Gu W et al. Osteogenic differentiation of bone marrow MSCs by β-tricalcium phosphate stimulating macrophages via BMP2 signalling pathway. *Biomaterials* 2014;35:1507–1518.
- 70 Gibson JD, O'Sullivan MB, Alaei F et al. Regeneration of articular cartilage by human ESC-derived mesenchymal progenitors treated sequentially with BMP-2 and Wnt5a. *STEM CELLS TRANSLATIONAL MEDICINE* 2017;6:40–50.
- 71 Ling L, Nurcombe V, Cool SM. Wnt signaling controls the fate of mesenchymal stem cells. *Gene* 2009;433:1–7.
- 72 Reis M, McDonald D, Nicholson L et al. Global phenotypic characterisation of human platelet lysate expanded MSCs by high-throughput flow cytometry. *Sci Rep* 2018;8:3907.
- 73 Heathman TR, Stolzing A, Fabian C et al. Serum-free process development: Improving the yield and consistency of human mesenchymal stromal cell production. *Cytotherapy* 2015;17:1524–1535.
- 74 Salzig D, Leber J, Merkwitz K et al. Attachment, growth, and detachment of human mesenchymal stem cells in a chemically defined medium. *Stem Cells Int* 2016;2016:1–10.
- 75 Leber J, Berekzai J, Blumenstock M et al. Microcarrier choice and bead-to-bead transfer for human mesenchymal stem cells in serum-containing and chemically defined media. *Process Biochem* 2017;59:255–265.